

**A Model for the Microstructure  
of Some Advanced Bainitic Steels**

M. Takahashi and H. K. D. H. Bhadeshia

Reprinted from

**MATERIALS TRANSACTIONS, JIM**

**VOL. 32 NO. 8, AUGUST, 1991**

**THE JAPAN INSTITUTE OF METALS**

**Aoba Aramaki, Aoba-ku, Sendai 980, Japan**

# A Model for the Microstructure of Some Advanced Bainitic Steels

M. Takahashi\* and H. K. D. H. Bhadeshia\*\*

Some applications of phase transformation theory towards the exploitation of bainitic microstructures are discussed, with particular emphasis on the quantitative aspects of alloying element effects. Examples are used to illustrate the principles involved in the design of advanced bainitic alloys of the type currently under investigation in the steel industry.

(Received March 25, 1991)

*Keywords: bainite, silicon steel, time-temperature-transformation curves, kinetics, thermodynamics*

## I. Introduction

Bainitic steels are now at the forefront of some potentially exciting developments in the steel industry, especially when the steels are destined for high-technology applications<sup>(1)-(15)</sup>. This, combined with recent advances in phase transformations theory, provides a unique opportunity for the development of fundamental alloy design procedures which could be used in the optimisation of candidate steels before they are fully commercialised.

In discussing bainitic steels, it is necessary to distinguish between two microstructural classes of bainitic steels. Although bainite is generally recognised to be a non-lamellar mixture of ferrite and carbides, the carbide precipitation reaction often lags behind the growth of bainitic ferrite, the time lag sometimes being so long that carbides are simply not found in the microstructure obtained by transformation within the bainite temperature range—the microstructure then consists of just bainitic ferrite and carbon-enriched residual austenite (together with any martensite which might form as the residual austenite is cooled to ambient temperature)<sup>(16)-(18)</sup>. A large number of bainitic alloys are used in a condition where carbides are not found in the microstructure, and this forms one of the classes of bainitic steels; the other is the more conventional microstructure in which carbide particles are found between the bainitic ferrite platelets, and in the case of lower bainite, within the platelets as well.

The purpose of the work presented here was to enable the solution of two theoretical problems, on the basis of current models on bainitic transformations:

- (i) the quantitative estimation of mixed microstructures of bainitic ferrite, austenite and martensite;
- (ii) the prediction of the onset of carbide precipitation during bainitic reaction. The complete problem is in fact quite formidable and only some aspects of it are addressed in this paper; Fig. 1 summarises the issues involved.

## II. Carbide-Free Bainitic Steels

It is an experimental fact that in steels where other reactions do not interfere (or occur simultaneously) with the growth of bainitic ferrite, the maximum volume fraction of ferrite that forms on prolonged holding at the isothermal transformation temperature is far below that expected on the basis of equilibrium or paraequilibrium transformation<sup>(17)(18)†</sup>. The important characteristic this *incomplete reaction phenomenon* is that the reaction stops well before the austenite achieves its paraequilibrium carbon concentration as given by the  $Ae'_3$  curve on the phase diagram<sup>(17)(18)</sup>. In fact, it stops when the carbon concentration of the residual austenite approaches the  $T_0$  curve, which describes the locus of all points on the phase diagram where austenite and ferrite of the same chemical composition have identical free energies. For bainite, whose growth is accompanied by an invariant-plane strain shape deformation, the strain energy of transformation is about  $400 \text{ J mol}^{-1}$ <sup>(23)</sup>, and the  $T_0$  curve as modified to account for this stored energy is called the  $T'_0$  curve.

A transformation in which carbon partitions during growth, and in which the mechanism of transformation is reconstructive (so that the product phase is not limited by austenite grain boundaries, and can grow to any size), can continue until the austenite achieves its equilibrium or paraequilibrium composition. Such a mechanism cannot therefore explain the observations described above. On the other hand, the incomplete reaction phenomenon can be understood if it is assumed that the bainitic ferrite grows without diffusion, with the carbon being partitioned into the residual austenite immediately after the growth event. As the austenite becomes progressively

\* R & D Laboratories-2, Nippon Steel Corporation, Chiba 299-12 Japan.

\*\* University of Cambridge/JRDC, Cambridge, U.K.

† Paraequilibrium<sup>(19)-(22)</sup> is a form of constrained equilibrium in which the iron-atom to substitutional-solute-atom ratio remains constant everywhere during transformation, but subject to that constraint, carbon achieves equality of chemical potential. For plain carbon steels, there is no difference between the paraequilibrium and equilibrium states. The  $Ae'_3$  phase boundary is thus the paraequilibrium equivalent of the  $Ae_3$  phase boundary of the Fe-C system.

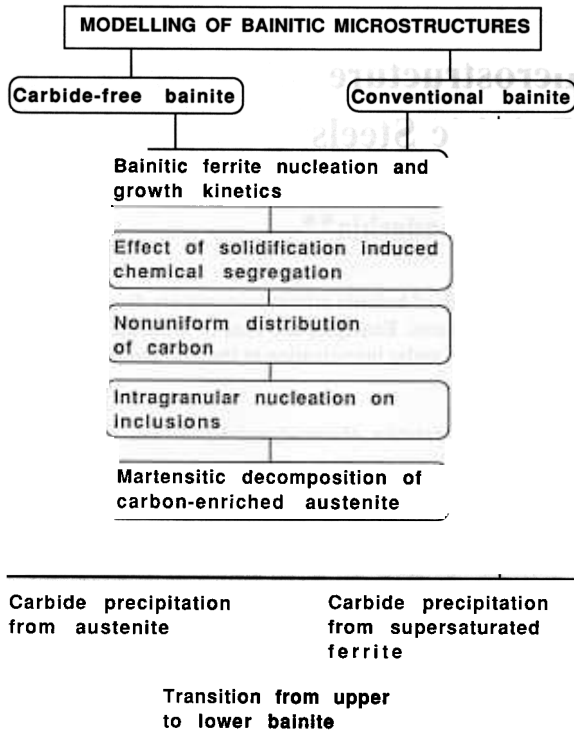


Fig. 1 Flow chart summarising the aspects of transformation which need to be addressed in order to be able to generally predict the microstructure of bainitic steels.

enriched with carbon, a stage is eventually reached when it is thermodynamically impossible for further bainite to grow by diffusionless transformation. At this point, the composition of the austenite is given by the  $T'_0$  curve of the phase diagram. This also explains why the degree of transformation to bainite is zero at the bainite-start ( $B_s$ ) temperature and increases with undercooling below  $B_s$ . The  $T'_0$  curve has a negative slope on a temperature/carbon concentration plot; the austenite can therefore tolerate more carbon as the temperature is reduced, before diffusionless transformation becomes impossible. The  $T_0$  and  $T'_0$  curves are in fact only slightly different in carbon concentration, and given that the carbon is often inhomogeneously distributed in the residual austenite<sup>(24)-(27)</sup>, it is a reasonable assumption to neglect the strain energy term in estimating the austenite composition when isothermal bainitic ferrite growth ceases.

### 1. Thermodynamics

As emphasised above, the incomplete reaction phenomenon can only be quantitatively assessed in steels where other reactions do not overlap with the formation of bainitic ferrite. These steels must obviously have a large enough bainitic hardenability and in addition should contain elements such as Al, Si, or Cr which retard the precipitation of cementite<sup>(28)-(33)</sup>. Many commercial alloys satisfy these conditions: ultrahigh-strength alloys such as "300M" steel, austempered ductile cast irons, forging steels, bainitic dual phase steels, etc. In all cases, their microstructures should consist of mixtures

of bainitic ferrite, retained austenite and martensite.

An established method of estimating the limiting volume fractions in such microstructures is based on the  $T_0$  concept<sup>(18)</sup>. This assumes that isothermal reaction is permitted for a time period  $t_c$  which is long enough to permit the volume fraction of bainitic ferrite to reach its limiting value. The effect of kinetic limitations is considered later.

The microstructure after isothermal transformation (at  $T_1$ ) in the upper bainite transformation range followed by cooling to ambient temperature ( $T_A$ ) consists of bainitic ferrite, carbon-enriched retained austenite and untempered martensite which forms during cooling from  $T_1 \rightarrow T_A$ . At  $T_1$ , the bainite reaction will cease when the carbon concentration of the residual austenite ( $x_\gamma$ ) approaches the  $T_0$  curve:

$$x_\gamma \rightarrow x_{T_0} \quad (1)$$

If the small difference in density between the ferrite and austenite is ignored, then the maximum volume fraction of bainitic ferrite (i.e.  $V_M$ ) is given by a lever rule applied to the  $Ae1'$  and  $T_0$  curves:

$$V_M = (x_{T_0} - \bar{x}) / (x_{T_0} - x^{\alpha\gamma} - x_C) \quad (2)$$

where  $x^{\alpha\gamma}$  is the paraequilibrium carbon concentration of the bainitic ferrite,  $\bar{x}$  the average carbon concentration of the alloys and  $x_C$  is the amount of carbon which is tied up as carbides within the bainitic ferrite.

On cooling the sample to ambient temperature, some of the residual austenite may transform to martensite with the remainder being retained. The martensite-start temperature ( $M_s$ ) of the residual austenite can be estimated by assuming that its carbon concentration is  $x_{T_0}$ , so that the amount of martensite ( $V_{\alpha'}$ ) that forms is given by Ref. (34):

$$V_{\alpha'} = (1 - V_M) [1 - \exp \{-0.011(M_s - T_A)\}] \quad (3)$$

Note that when dealing with upper bainite, the method permits the calculation of the volume fractions of all the phases and also their detailed chemical compositions. There is unfortunately, no method for predicting  $x_C$ , so that similar calculations for lower bainite are not yet possible. The method also assumes that the partitioned carbon is distributed homogeneously within the residual austenite. No account is taken of the fact that many industrial alloys are chemically heterogeneous.

Some new published data are available for comparison against the  $T_0$  criterion. The lattice parameters of austenite retained in Fe-0.2C-1.5Si mass% alloys containing varying concentrations of manganese have been measured using X-ray diffraction by Usui *et al.*<sup>(35)</sup> Since carbon in solid solution causes an expansion of the austenite lattice parameter, these data can be used to deduce the carbon concentration of the retained austenite. Taking the relationship between the lattice parameter and  $x_\gamma$  to be given by Ref. (36):

$$a_\gamma = 0.3573 + 0.00075x_\gamma \text{ nm}$$

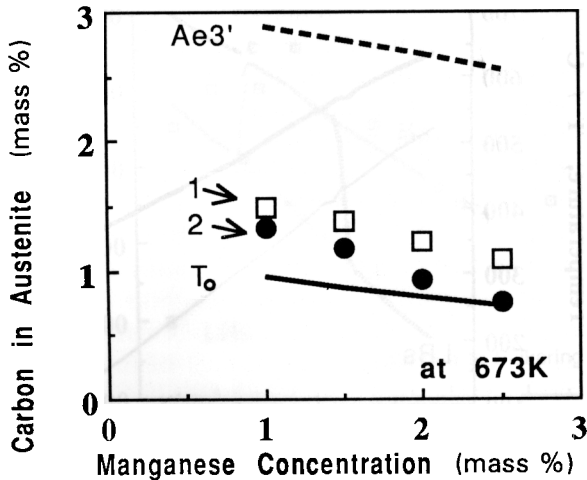


Fig. 2 An analysis of published data<sup>(35)</sup> on the carbon concentration of retained austenite in a mixed microstructure of bainitic ferrite, martensite and retained austenite. The calculations of the  $Ae3'$  and  $T_0$  curves were carried out as described in Ref. (11), (12). Usui *et al.*<sup>(35)</sup> measured the lattice parameter of austenite and used a relationship between the parameter and carbon concentration to deduce the data illustrated by curve 1. A better parameter/carbon relation is used here to generate curve 2. It is evident that there is good agreement of the austenite composition with that predicted by the  $T_0$  calculations.

it is found that the calculated compositions of the retained austenite agree well with the calculated  $T_0$  curves (Fig. 2), and the effect of manganese is also well represented by the thermodynamically calculated  $T_0$  curves.

## 2. Kinetics

Many industrial heat-treatments involve isothermal transformation for time periods less than those required to allow the bainite reaction to reach completion. It is often the case that the heat-treatment utilised is not isothermal. The thermodynamic approach described above fails in both of these circumstances. To correctly treat such cases, it is necessary to be able to predict the appropriate time-temperature-transformation (TTT) and continuous-cooling-transformation diagrams for bainite.

Bhadeshia has presented a method<sup>(37)</sup>, based on Russell's expression for incubation time during nucleation<sup>(38)(39)</sup>, for estimating the TTT diagram of multi-component steels. The TTT diagram is considered to consist essentially of two 'C'-curves, the high temperature curve representing reconstructive reactions such as allotriomorphic ferrite and pearlite, the lower temperature curve representing displacive transformations such as Widmanstätten ferrite and bainite. Most of the features of published TTT diagrams for steels can be understood via the different effects of alloying elements on these two C-curves. The original paper however, dealt with just a prediction of the incubation period prior to the onset of transformation at each temperature (i.e. the curves representing the initiation of a detectable degree of transformation). This is of course inadequate for the present requirements but the method can be adapted to predict the whole family of C-curves representing the

progress of bainitic reaction in a particular steel, as described below.

In the original model<sup>(37)</sup>, the incubation time  $\tau_s$  for the beginning of transformation is given by:

$$\ln \{ \tau_s G_{\max}^p T^{-z} \} = (Q'/RT) + C_4 \quad (4)$$

where  $p$ ,  $z$ ,  $Q'$  and  $C_4$  are constants obtained by fitting to experimental data,  $G_{\max}$  represents the maximum driving force available for nucleation and  $\tau$  represents the incubation time prior to the formation of a detectable degree of transformation product. As the bainite reaction proceeds beyond this initial stage, the austenite becomes enriched with carbon. The degree of enrichment can easily be calculated using the mass balance condition. In the present work, bainite C-curves representing further degrees of reaction are calculated by applying eq. (4) to enriched austenite, with  $G_{\max}$  depending on the new composition of the austenite.

Scheil's rule<sup>(40)</sup> is then used to convert the TTT diagram into a CCT diagram. It is therefore assumed that the additivity principle applies to each of the C-curves in the TTT diagram, with the specified degree of transformation being achieved if

$$\int_0^t \Delta t / \tau_f \{ T \} = 1 \quad (5)$$

where  $\tau_f \{ T \}$  is the incubation time at temperature  $T$  for the C-curve representing a fraction  $f$  of reaction,  $\Delta t$  is the time interval spent by the sample at the temperature  $T$ , and  $t$  is the time defined to be zero above the bainite-start temperature.

Typical calculations, for a series of low alloy silicon-rich steels are presented in Fig. 3. Note that they do not allow for the formation of lower bainite, for the solidification-induced chemical segregation that is inevitably present in commercial alloys, the effects on inhomogeneous carbon distributions, etc. The calculations are in this sense, unrealistic, but the trends that they indicate should be correct.

## III. Carbide Precipitation from Bainitic Ferrite

As discussed earlier, the growth of bainite is probably diffusionless, but any excess carbon in the supersaturated ferrite soon afterwards partitions into the residual austenite or precipitates within the bainitic ferrite in the form of carbides. When the process of carbon partitioning into the residual austenite is rapid relative to that of carbide precipitation, the transformation product is called "upper bainite", whereas "lower bainite" is obtained when some of the carbon supersaturation is relieved by precipitation within the bainitic ferrite.

The transition from upper to lower bainite can therefore be estimated by comparing the time  $t_d$  required to partition excess carbon into austenite, with the time  $t_c$  necessary to achieve a detectable degree of carbide precipitation within the ferrite<sup>(41)</sup>. The diffusion time is given by:

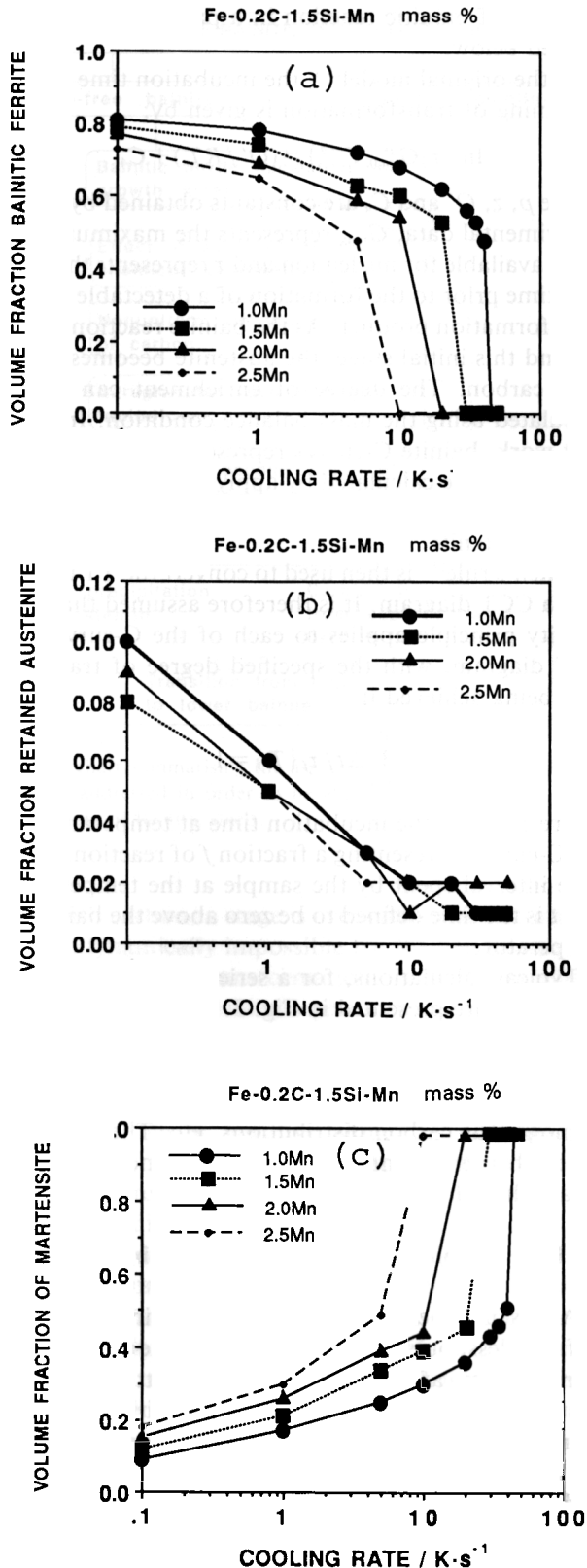


Fig. 3 Typical calculated microstructure for a series of Fe-Mn-Si-C alloys.

$$t_d \approx \frac{\omega^2 \pi (\bar{x} - x^{\alpha\gamma})^2}{16D(x^{\gamma\alpha} - \bar{x})} \quad (6)$$

where  $\bar{x}$  is the average carbon concentration in the steel as a whole,  $x^{\alpha\gamma}$  and  $x^{\gamma\alpha}$  are the carbon concentrations in the

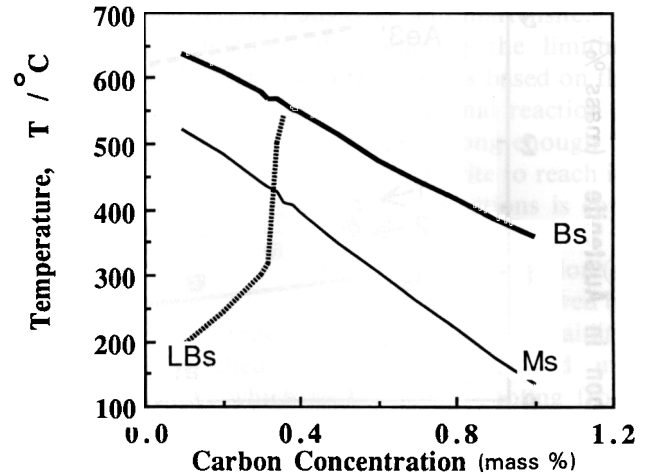


Fig. 4 Prediction of the upper to lower bainite transition temperature as a function of the carbon concentration for a series of plain carbon steels<sup>(44)</sup>.  $B_s$ ,  $L_s$  and  $M_s$  represent the bainite-start, lower bainite-start and martensite-start temperatures. Both calculation and theory seem to indicate that only upper bainite is obtained with the carbon concentration for Fe-C alloys is less than about 0.4 mass%, and only lower bainite when that concentration is exceeded.

ferrite and austenite which are in paraequilibrium,  $\omega$  is the thickness of the bainitic ferrite platelet, and  $D$  is a weighted average carbon diffusivity in austenite<sup>(42)(43)</sup>.

Although there is as yet no rigorous model capable of predicting the kinetics of carbide precipitation from supersaturated ferrite, it is possible to fit Avrami type relationships to martensite tempering data and estimate the time period  $t_c$ <sup>(44)</sup>, and consequently, by comparing  $t_d$  and  $t_c$ , the upper to lower bainite transition temperature  $T_{LB}$ . Using this method, it has been demonstrated that there is a maximum in  $T_{LB}$  as a function of carbon concentration at around 0.4 mass% carbon (Fig. 4) in Fe-C alloys. It is further predicted that in plain carbon steels, only upper bainite can be obtained before the onset of martensitic transformation, followed by a narrow range of carbon in which both upper and lower bainite are possible, and as the carbon concentration is increased ( $>0.4$  mass% C), only lower bainite and martensite can be obtained during heat treatment at temperatures below that at which pearlite forms<sup>(44)</sup>. These predictions, together with the position of the peak and the shape of the transition curve are in fact broadly consistent with published experimental data on plain carbon steels, although there are outstanding difficulties as indicated in Ref. (44).

On applying this model<sup>(44)</sup> to experimental data on Fe-Mo-Mn-C alloys<sup>(45)</sup>, without taking account of any effect of the molybdenum or manganese on carbide precipitation kinetics, good agreement between theory and experiment is once again obtained (Fig. 5).

#### IV. Cementite Precipitation from Supersaturated Austenite

Austenite is supersaturated with respect to cementite

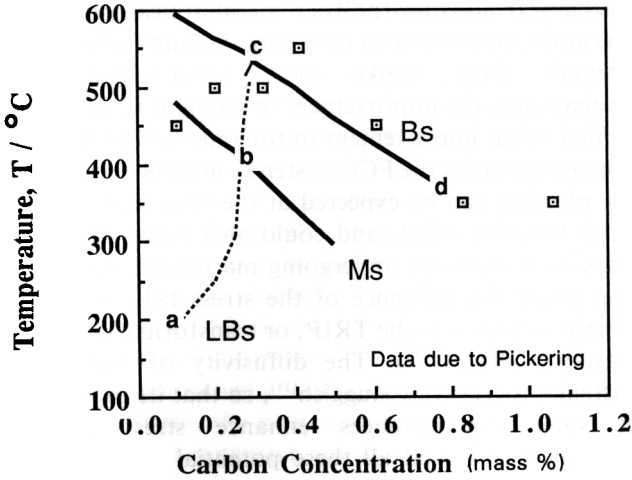


Fig. 5 Effect of carbon concentration on the temperature for the upper to lower bainite transition in Fe-Mn-Mo-C alloys. The points represent experimentally measured transition temperatures due to Pickering<sup>(45)</sup> whereas the curve “abcd” represents the calculated transition temperature as a function of carbon concentration. Beyond about 0.3 wt% C, the bainite obtained is always lower bainite.

( $\theta$ ) precipitation when  $x^{\gamma} > x^{\gamma\theta}$ ; for the bainite reaction, this means that  $x_{T_0} > x^{\gamma\theta}$  since the growth of bainitic ferrite stops when  $x^{\gamma}$  reaches the value  $x_{T_0}$  given by the  $T_0$  curve of the phase diagram. A consequence of the precipitation of cementite from austenite is that its carbon concentration drops below  $x_{T_0}$ , so that the growth of bainitic ferrite can continue to an extent larger than would be otherwise possible. It is therefore important to be able to predict the kinetics of cementite precipitation from the residual austenite, and the problem is one of nucleation and growth of cementite.

Assuming that the cementite forms by reconstructive transformation (the actual mechanism has yet to be established), the incubation time  $\tau$  for nucleation can be estimated using Russell’s model<sup>(38)(39)</sup>. The incubation time should decrease as the magnitude of the maximum driving force for nucleation,  $G_{max}$ , increases (see eq. (4)). Our calculations based on the assumption that the nuclei form with the equilibrium composition, indicate that the retardation of cementite precipitation by silicon cannot

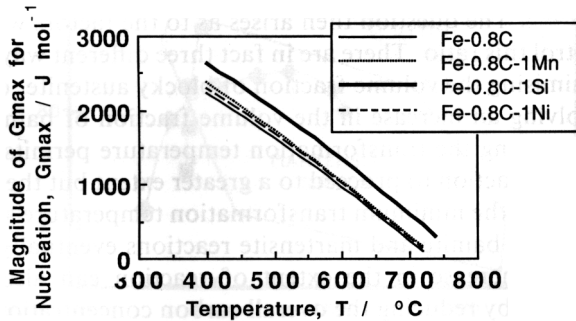


Fig. 6 Calculated maximum free energy change ( $G_{max}$ ) due to the nucleation of cementite from austenite in Fe-0.8C-X mass% ternary alloys, assuming that the cementite nuclei have the equilibrium composition.

be related to the nucleation stage, since silicon is actually found to increase  $G_{max}$ —Fig. 6.

1. Effect of alloying elements on cementite growth

The growth rate is here estimated using the theory of diffusion-controlled interfacial motion. Since the cementite particles found in bainitic microstructures are plate shaped and usually have large aspect ratios, it may be a good approximation to represent the formation of these plates using a one-dimensional parabolic thickening rate constant ( $\alpha_1$ ), so that the plates are essentially treated here as allotriomorphs. It is further assumed that any concentration gradients can be approximated as being constant (after Zener) and the problem is studied for ternary Fe-C-X alloys, where “X” denotes a substitutional solute; C and X are in the equations that follow, identified using the subscripts 1 and 2 respectively. When local equilibrium is assumed to exist at the transformation interface, it can be demonstrated using the methods of Kirkaldy and Coates<sup>(46)(47)</sup> that the parabolic thickening rate constant can be obtained from the simultaneous solution of the following equations:

$$\alpha_1^2 = D_{11} \frac{(x_1^{\gamma} - x_1^{\gamma\theta})^2}{(x_1^{\theta\gamma} - x_1^{\gamma})(x_1^{\theta\gamma} - x_1^{\gamma\theta})} + D_{12} \frac{(x_2^{\gamma} - x_2^{\gamma\theta})^2}{(x_2^{\theta\gamma} - x_2^{\gamma})(x_2^{\theta\gamma} - x_2^{\gamma\theta})} \quad (7)$$

$$\alpha_1^2 = D_{22} \frac{(x_2^{\gamma} - x_2^{\gamma\theta})^2}{(x_2^{\theta\gamma} - x_2^{\gamma})(x_2^{\theta\gamma} - x_2^{\gamma\theta})} \quad (8)$$

where  $x_1^{\gamma}$  and  $x_2^{\gamma}$  represent the average composition of the austenite, and  $x_1^{\theta\gamma}$  and  $x_2^{\theta\gamma}$  the equilibrium compositions of the cementite and austenite respectively.  $D_{11}$  is the weighted average diffusivity of carbon in the austenite,  $D_{12}$  represents the dependence of the carbon flux in austenite on the concentration gradient of the substitutional solute, and  $D_{22}$  the diffusivity of the substitutional solute in the austenite. The diffusion coefficient  $D_{12}$  is given by

$$D_{12} = D_{11} \frac{\epsilon_{12}x_1^{\gamma}}{1 + \epsilon_{11}x_1^{\gamma}} \quad (9)$$

where the  $\epsilon$  terms are the Wagner interaction parameters which arise in dilute solid solution models, as discussed elsewhere<sup>(48)</sup>. It is assumed that the composition of the growing cementite is uniform everywhere.

It is also possible that the cementite grows with para-equilibrium, in which case the iron atom to substitutional solute atom ratio should be constant everywhere. The rate constant is then given by:

$$\alpha_1^2 = D_{11} \frac{(x_1^{\gamma} - x_1^{\gamma\theta})^2}{(x_1^{\theta\gamma} - x_1^{\gamma})(x_1^{\theta\gamma} - x_1^{\gamma\theta})} \quad (10)$$

Note that the concentration terms  $x_1^{\theta\gamma}$  and  $x_1^{\gamma\theta}$  now represent *paraequilibrium* rather than equilibrium compositions of the two phases.

Figure 7 shows the results of growth rate calculations, carried out assuming paraequilibrium growth of cementite from austenite (consistent with experimental data—Ref. (18)). It is evident that the growth of cementite is substantially retarded by silicon.

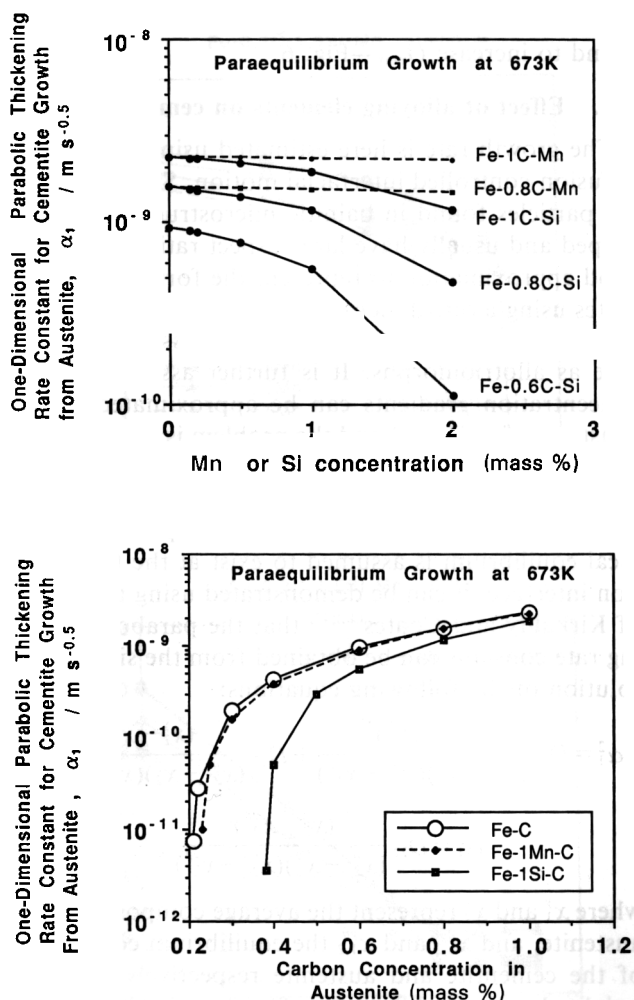


fig. 7 Parabolic thickening rate constants for the paraequilibrium growth of cementite allotriomorphs from austenite.

## V Stability of Austenite & Effect on Properties

The mixture of bainitic ferrite and austenite is in principle an ideal combination from many points of view<sup>(11)-(15)</sup>. Most modern high-strength steels are clean in the sense that they are largely free from nonmetallic inclusions. Those destined for critical applications are usually vacuum arc refined prior to fabrication and heat-treatment. As a consequence, it is the components of the intrinsic microstructure, such as particles of cementite, which are responsible for damage initiation. The upper bainitic ferrite and austenite mixture is however, free from cleavage and void nucleating cementite. The ferrite also has a very low interstitial content, since much of the excess carbon is partitioned into the residual austenite; the toughness of ferrite is known to deteriorate rapidly with an increasing concentration of carbon in solid solution.

The microstructure derives its strength from the ultrafine grain size which results from the displacive mechanism of ferrite growth, giving an effective grain size which is much less than 1  $\mu\text{m}$ . Such a small grain size cannot be achieved by any commercial process other than

mechanical alloying (powder metallurgical process). A fine grain structure is an optimum method for improving strength since unlike most other strengthening mechanisms, the improvement in strength is also accompanied by an improvement in toughness. The intimately dispersed and ductile FCC austenite films between the ferrite platelets can be expected at the very least to have a crack blunting effect, and could also make increase the work of fracture by undergoing martensitic transformation under the influence of the stress field of the propagating crack (i.e. the TRIP, or transformation induced plasticity effect<sup>(49)(50)</sup>). The diffusivity of hydrogen in austenite is relatively sluggish<sup>(51)</sup>, so that its presence can in some circumstances enhance stress corrosion resistance<sup>(52)(53)</sup>. And all these potential benefits can be achieved by creating a duplex microstructure with the cheapest austenite stabiliser available, carbon, whose concentration in the austenite is enhanced during transformation, so that the average carbon concentration of the steel need not be large.

In spite of all these potential advantages, the bainitic ferrite/austenite microstructure has on many occasions failed to live up to its promise<sup>(11)-(15)(54)</sup>, primarily because of the instability of relatively large or blocky regions of austenite which become trapped between sheaves of bainite. The blocks of austenite tend to transform to high-carbon, untempered martensite under the influence of small stresses and consequently have an embrittling effect. The films of austenite that are trapped between the platelets of ferrite in a sheaf are much more stable, partly because of their higher carbon concentration, and also because of the physical constraint to transformation due to the close proximity of plates in all directions.

If it is assumed that a fraction  $\phi$  of a sheaf consists of films of austenite, then it can be demonstrated that the ratio of the volume fractions of film and blocky austenite (prior to any martensitic transformation) is given by:

$$V^{\gamma-F} / V^{\gamma-B} = (\phi V^\alpha) / (V^\gamma - \phi V^\alpha) \quad (11)$$

where  $V^{\gamma-F}$  and  $V^{\gamma-B}$  are the volume fractions of film and blocky type retained austenite respectively, and  $V^\alpha$  and  $V^\gamma$  the total volume fractions of bainitic ferrite and residual austenite respectively. It is found experimentally that high strength and good toughness can be obtained by maintaining the above ratio to a value greater than 0.9<sup>(11)(12)</sup>. The question then arises as to the factors which control this ratio. There are in fact three different ways of minimising the volume fraction of blocky austenite, each involving an increase in the volume fraction of bainite.

Lowering the transformation temperature permits the bainite reaction to proceed to a greater extent but there is a limit to the minimum transformation temperature since the lower bainite and martensite reactions eventually set in. An increase in the extent of reaction can also be achieved by reducing the overall carbon concentration of the steel, so that the austenite reaches its limiting composition at a later stage of the reaction. The  $T_0$  curves of the phase diagram, which determine the composition of the austenite at the point where the reaction stops, can

also be shifted to higher carbon concentrations by altering the substitutional solute concentration of the steel. The effect on toughness in reducing the amount of blocky austenite is very pronounced, with large reductions in the impact transition temperatures as the ratio of film to blocky austenite is increased in the manner just described. Note that for a duplex  $\alpha + \gamma$  microstructure, the strength actually increases as the fraction of bainitic ferrite increases, so that the better toughness is obtained without sacrificing strength. Typical compositions of high-strength steels which show good toughness are given in Table 1. Figure 8 shows how the mechanical properties compare with quenched and tempered steels. It is evident that in some cases, the properties match those obtained from much more expensive maraging steels.

The properties of these steels improve only slightly when tempered at temperatures not much higher than the transformation temperature at which the original bainite formed. However, annealing at elevated temperatures or prolonged periods at low temperatures can lead to the decomposition of the austenite into ferrite and carbides, with a simultaneous drop in strength and toughness, especially the upper shelf energy. The latter effect can be attributed directly to the void nucleating propensity of carbide particles in the tempered microstructure, as illustrated by the much smaller void size evident in the fracture surface of the tempered sample.

The mechanical property data on these high silicon steels, especially those steels designed using the phase transformation theory discussed earlier, look extremely

promising. It is however, unlikely that the experimental steels represent the optimum compositions and further development work could lead to even better properties. It is also necessary to carry out a comprehensive assessment of properties such as stress corrosion resistance, fatigue etc.

### 1. Ductility

The influence of retained austenite on ductility has been studied mainly in steels containing a high silicon concentration, where cementite formation can be prevented, and consequently large quantities of carbon-enriched austenite can be retained. Ductility as measured by tensile elongation, reaches a peak (optimum) value as a function of the volume fraction of retained austenite, when the amount of austenite is varied by altering the volume fraction of isothermal transformation to bainite<sup>(55)</sup>. Furthermore, the uniform elongation behaves in a similar way to total elongation when plotted against the volume fraction of retained austenite. The difference between the uniform and total elongation decreases as the optimum volume fraction of retained austenite is reached; beyond the optimum value, tensile failure occurs before the necking instability so that the difference between uniform and total elongations vanishes.

It seems that the best elongation behaviour is observed when the retained austenite is present mainly in the form of films between the sub-units of bainite, rather than as blocky regions between the sheaves of bainite<sup>(55)</sup>. Hence, the optimum retained austenite content increases as the transformation temperature decreases, because the sub-unit thickness decreases, permitting more of the austenite to be in the film morphology for a given volume fraction of transformation to bainite. For the same reason, the elongation becomes less sensitive to retained austenite content as the transformation temperature is reduced. While mechanically unstable austenite, i.e. the austenite which decomposes to deformation induced martensite, is recognised to cause a deterioration in toughness for bainitic steels<sup>(11)(12)(54)</sup>, this is not the case for ductility, presumably because of the TRIP effect and the lower strain rates involved in conventional tensile tests.

It must be emphasised that all these results are very difficult to interpret quantitatively. Changes in retained austenite content cannot easily be made without altering other factors such as the tensile strength and the distribution of the austenite. For example, Miihkinen and Edmonds<sup>(14)</sup> have reported a monotonic increase in uniform and total ductility with retained austenite content. The latter was varied by altering the transformation temperature, so that the strength increased as the austenite content decreased.

Table 1 Chemical compositions (mass%) of some successful alloys based on a mixed microstructure of bainitic ferrite and austenite.

C	Si	Mn	Ni
0.22	2.0	3.0	—
0.40	2.0	—	4.0

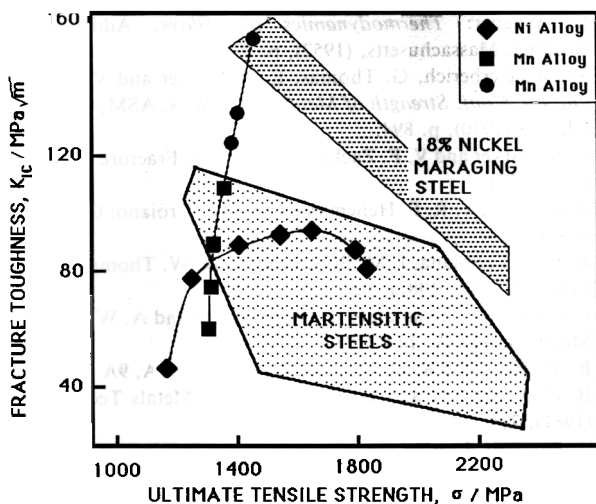


Fig. 8 Comparison of the mechanical properties of mixed microstructure of bainitic ferrite and austenite, versus those of quenched and tempered martensitic alloys<sup>(15)</sup>.

## VI. Summary & Future Work

A start has been made on the complicated problem of predicting the microstructure of bainitic steels, by developing an approximate method of calculating the time-temperature-transformation diagram for the forma-



tion of bainite. There remain significant difficulties: future work will have to address the problem of chemical segregation, nonuniform distribution of carbon in any residual austenite, more complete models for carbide precipitation during bainitic transformation, and other problems highlighted in Fig. 1. It should nevertheless be possible to give good hints on the expected changes of microstructure and mechanical properties as alloy chemistry and thermal treatments are varied. Steady progress is also being made in evaluating the relationships between microstructure and mechanical properties, although more research is needed to establish these on a quantitative basis.

#### Acknowledgments

We are grateful to the Nippon Steel Corporation and to Professor C. J. Humphreys (University of Cambridge) for the provision of laboratory facilities. HKDHB's contribution to this work was carried out under the auspices of the "Atomic Arrangements: Design and Control" project, which is a collaborative venture between the Research and Development Corporation of Japan and the University of Cambridge.

#### REFERENCES

- (1) O. Matsumura, Y. Sakuma and H. Takechi: *Trans. ISIJ*, **27** (1987), 570.
- (2) O. Matsumura, Y. Sakuma and H. Takechi: *Scripta Metall.*, **21** (1987), 1301.
- (3) S. Bandoh, O. Matsumura and Y. Sakuma: *Trans. ISIJ*, **28** (1988), 569.
- (4) M. Imagumbai, R. Chijiwa, N. Aikawa, M. Nagumo, H. Homma, S. Matsuda and H. Mimura: *HSLA Steels: Metallurgy and Applications*, ed. by J. M. Gray, T. Ko, Z. Shouhua, W. Baorong and X. Xishan, ASM International, Ohio, (1985), p. 557.
- (5) K. Yamamoto, S. Matsuda, T. Haze, R. Chijiwa and H. Mimura: *Residual and Unspecified Elements in Steel*, ASM International, Ohio, (November 1987), p. 1.
- (6) R. Chijiwa, H. Tamehiro, M. Hirai, H. Matsuda and H. Mimura: *Offshore Mechanics and Arctic Engineering Conference (OMAE)*, Houston, Texas, (1988), p. 1.
- (7) K. Nishioka and H. Tamehiro: *Microalloying '88: International Symposium on Applications of HSLA Steel*, Chicago, Illinois, (September 1988), p. 1.
- (8) H. K. D. H. Bhadeshia: *Steel Technology International*, ed. by P. H. Scholes, Sterling Publications International Ltd., London, (1989), p. 289.
- (9) Y. Tomita and K. Okabayashi: *Metall. Trans. A*, **14A** (1983), 485.
- (10) Y. Tomita and K. Okabayashi: *Metall. Trans. A*, **16A** (1985), 73.
- (11) H. K. D. H. Bhadeshia and D. V. Edmonds: *Metal. Sci.*, **17** (1983), 411.
- (12) H. K. D. H. Bhadeshia and D. V. Edmonds: *Metal Sci.*, **17** (1983), 420.
- (13) V. T. T. Miihkinen and D. V. Edmonds: *Mater. Sci. and Tech.*, **3** (1987), 422.
- (14) V. T. T. Miihkinen and D. V. Edmonds: *Mater. Sci. and Tech.*, **3** (1987), 432.
- (15) V. T. T. Miihkinen and D. V. Edmonds: *Mater. Sci. and Tech.*, **3** (1987), 441.
- (16) R. F. Hehemann: *Phase Transformations*, ASM, Metals Park, OH, (1970), p. 397.
- (17) J. W. Christian and D. V. Edmonds: *Int. Conf. on Phase Transformations in Ferrous Alloys*, ed. by A. R. Marder and J. I. Goldstein, TMS-AIME, Warrendale, PA, (1984), p. 293.
- (18) H. K. D. H. Bhadeshia and J. W. Christian: *Metall. Trans. A*, **21A** (1990), 767.
- (19) A. Hultgren: *Trans. ASM*, **39** (1947), 915.
- (20) A. Hultgren: *Jernkontorets Ann.*, **135** (1951), 403.
- (21) M. Hillert: *Jernkontorets Ann.*, **135** (1951), 25.
- (22) E. Rudberg: *Jernkontorets Ann.*, **136** (1952), 91.
- (23) H. K. D. H. Bhadeshia: *Acta Metall.* **29** (1981), 1117.
- (24) S. J. Matas and R. F. Hehemann: *Trans. Met. Soc. AIME*, **221** (1961), 179.
- (25) A. Schrader and F. Wever: *Arch. Eisenhütt.*, **23** (1952), 489.
- (26) H. K. D. H. Bhadeshia and A. R. Waugh: *Acta Metall.*, **30** (1982), 775.
- (27) I. Stark, G. D. W. Smith and H. K. D. H. Bhadeshia: *Phase Transformations '87*, ed. by G. W. Lorimer, Institute of Metals, London, (1988), p. 211.
- (28) E. C. Bain: *Alloying Elements in Steel*, ASM, Cleveland, OH, (1939), p. 68.
- (29) W. S. Owen: *Trans. ASM*, **46** (1954), 812.
- (30) J. Gordine and I. Codd: *J. Iron Steel Inst.*, **207.1** (1969), 461.
- (31) R. M. Hobbs, G. W. Lorimer, N. Ridley: *J. Iron Steel Inst.*, **210.2** (1972), 757.
- (32) A. G. Alten and P. Payson: *Trans. ASM*, **45** (1953), 498.
- (33) E. E. Langer: *Metal Sci. J.*, **2** (1968), 59.
- (34) P. P. Koistinen and R. E. Marburger: *Acta Metall.*, **7** (1959), 59.
- (35) N. Usui, K. Sugimoto, E. Nishida, M. Kobayashi and S. Hashimoto: *CAMP-ISIJ*, **3** (1990), 2013.
- (36) L. Cheng, A. Bottger, Th. H. de Keijseer and E. J. Mittermeijer: *Scripta Met.*, **24** (1990), 509.
- (37) H. K. D. H. Bhadeshia: *Metal Sci.*, **16** (1982), 159.
- (38) K. C. Russell: *Acta Metall.*, **16** (1968), 761.
- (39) K. C. Russell: *Acta Metall.*, **17** (1969), 1123.
- (40) J. W. Christian: *Theory of Transformations in Metals and Alloys*, Part I, 2nd edition, Pergamon Press, Oxford, (1975), p. 525.
- (41) H. K. D. H. Bhadeshia: *Phase Transformation '87*, ed. by G. W. Lorimer, Inst. of Metals, London, (1988), p. 309.
- (42) R. H. Siller and R. B. McLellan: *Metall. Trans. A*, **1** (1970), 985.
- (43) H. K. D. H. Bhadeshia: *Metal Sci.*, **15** (1981), 477.
- (44) M. Takahashi and H. K. D. H. Bhadeshia: *Mater. Sci. and Tech.*, **6** (1990), 592.
- (45) F. B. Pickering: *Transformation and Hardenability in Steels*, Climax Molybdenum Co., Ann Arbor, MI, (1967), p. 109.
- (46) J. S. Kirkaldy: *Canadian Journal of Physics*, **36** (1958), 899.
- (47) D. E. Coates: *Metall. Trans.*, **3** (1972), 1203.
- (48) C. Wagner: *Thermodynamics of Alloys*, Addison-Wesley, Reading, Massachusetts, (1952), p. 53.
- (49) W. W. Gerberich, G. Thomas, E. R. Parker and V. F. Zackay: *2nd Int. Conf. Strength of Metals and Alloys*, ASM, Metals Park, Ohio, **3** (1970), p. 894.
- (50) E. R. Parker and V. F. Zackay: *Engineering Fracture Mechanics*, **7** (1975), 371.
- (51) J. H. Shievely, R. F. Hehemann and A. R. Troiano: *Corrosion*, **22** (1966), 253.
- (52) R. Kerr, F. Solana, I. M. Bernstein and A. W. Thompson: *Metall. Trans. A*, **18A** (1987), 1011.
- (53) F. Solana, C. Takamatate, I. M. Bernstein and A. W. Thompson: *Metall. Trans. A*, **18A** (1987), 1023.
- (54) R. M. Horn and R. O. Ritchie: *Metall. Trans. A*, **9A** (1978), 1039.
- (55) B. P. J. Sandvik and H. P. Nevalainen: *Metals Technology*, **13** (1981), 213.